

Analytical expressions for stopping-power ratios relevant for accurate dosimetry in particle therapy

Armin Lühr^{1,2}, David C. Hansen², Oliver Jäkel^{3,4}, Nikolai Sobolevsky⁵, and Niels Bassler^{1,2}

¹ Department of Experimental Clinical Oncology, Aarhus University Hospital, Aarhus, Denmark

² Department of Physics and Astronomy, University of Aarhus, Aarhus, Denmark

³ Department of Medical Physics in Radiation Oncology, German Cancer Research Center (DKFZ), Heidelberg, Germany

⁴ Heidelberg Ion Beam Therapy Center (HIT), Heidelberg University Hospital, Heidelberg, Germany

⁵ Department of Neutron Research, Institute for Nuclear Research of the Russian Academy of Sciences, Moscow 117312, Russia

E-mail: luehr@phys.au.dk; bassler@phys.au.dk

Abstract

Abstract. In particle therapy, knowledge of the stopping-power ratios (STPRs) of the ion beam for air and water is necessary for accurate ionization chamber dosimetry. Earlier work has investigated the STPRs for pristine carbon ion beams, but here we expand the calculations to a range of ions ($1 \leq z \leq 18$) as well as spread out Bragg peaks (SOBPs) and provide a theoretical in-depth study with a special focus on the parameter regime relevant for particle therapy.

The Monte Carlo transport code SHIELD-HIT is used to calculate complete particle-fluence spectra which are required for determining STPRs according to the recommendations of the International Atomic Energy Agency (IAEA).

We confirm that the STPR depends primarily on the current energy of the ions rather than on their charge z or absolute position in the medium. However, STPRs for different sets of stopping-power data for water and air recommended by the International Commission on Radiation Units & Measurements (ICRU) are compared, including also the recently revised data for water, yielding deviations up to 2% in the plateau region. In comparison, the influence of the secondary particle spectra on the STPR is about two orders of magnitude smaller in the whole region up till the practical range. The gained insights enable us to propose an analytic approximation for the STPR for both pristine and SOBPs as a function of penetration depth, which parametrically depend only on the initial energy and the residual range of the ion, respectively.

PACS numbers: 87.55.Qr, 34.50.Bw, 87.53.Bn, 87.55.K-

1. Introduction

Stopping powers are essential for calculating the dose deposited by ionizing particles. The deposited dose is described as the mass stopping power multiplied with the particle fluence, while assuming charged particle equilibrium from the short-ranged delta electrons. At particle-therapy centers air-filled ionization chambers are routinely used as a main tool for quality assurance of the delivered beam. Several dosimetry protocols for protons have been conceived and the most recent protocols provided by the International Commission on Radiation Units and Measurements (ICRU) and International Atomic Energy Agency (IAEA), ICRU 59 [1] and TRS-398 [2], respectively, set the standard in proton dosimetry today. In addition, TRS-398 also covers dosimetry for ions heavier than protons. Both protocols use an absorbed dose-to-water based formalism and relate the dose to water $D_{w,Q}$ to the acquired charge M_Q multiplied by a calibration factor N_{D,w,Q_0} and a dimensionless beam quality correction factor k_{Q,Q_0} . The correction factor k_{Q,Q_0} relates the measured beam quality Q to the beam quality Q_0 used for calibration of the dosimeter. It is defined in different ways in ICRU 59 and TRS-398, more specifically TRS-398 includes a perturbation factor p_Q/p_{Q_0} which considers effects for the specific ionization chamber used. The beam quality correction factor in TRS-398,

$$k_{Q,Q_0} = \frac{(S_{\text{water/air}})_Q}{(S_{\text{water/air}})_{Q_0}} \frac{(W_{\text{air}})_Q}{(W_{\text{air}})_{Q_0}} \frac{p_Q}{p_{Q_0}} \quad (1)$$

following Bragg-Gray cavity theory, includes the stopping-power ratio of water to air, $S_{\text{water/air}}$, and the mean energy expended in air per ion pair formed, W_{air} .

As mentioned in TRS-398, calculating the correct beam quality factor in particle therapy is difficult since it involves knowledge of the entire particle-energy spectrum. Instead, TRS-398 proposes a pragmatic approach by recommending a fixed value of 1.13 as a generic correction factor for the dosimetry of ions heavier than protons based on the analysis by Hartmann *et al.* [3], irrespective of the particle types and energy spectra which are functions of depth. Accordingly, TRS-398 summarizes that the estimated combined standard uncertainty in k_{Q,Q_0} in ion beams heavier than protons (about 3%) arises largely from the uncertainty of the stopping-power ratio (STPR) (about 2%) and the value for W_{air} (about 1.5%).[‡] This has been taken up by Henkner *et al.* [4] and Geithner *et al.* [5, 6] for mono energetic *carbon* beams, and they found out that (i) the STPR is not constant but varies with penetration depth, and (ii) it depends strongly on the accuracy of the stopping-power data used as input for the calculation. Accordingly, it was concluded that in a clinical setting an over or under dosage may occur in the order of a few percent.

Here, we shall continue the initiated work on STPRs focusing on two objectives. First, gaining a sound understanding of the physics which determine the STPR, and second, exploiting the gained understanding in order to provide results with direct

[‡] Although the study of the value for W_{air} is beyond the scope of this work it shall be mentioned that the estimated uncertainty for W_{air} calls for a detailed investigation.

clinical relevance which are ready to be applied in clinical practice in a quality assurance setting.

The deeper insight in the context of STPR is required since STPR strongly depends on the stopping-power data which are used for its determination. The problem is, however, that the stopping-power data currently recommended by ICRU possess some intrinsic inconsistencies. In contrast to a accurate but purely numerical calculation of STPRs, a sound understanding of the relevant physics allows for conclusions independent of the employed set of stopping-power data. It is also a prerequisite for a functional description of the STPR. It should be emphasized that, in contrast to earlier work on STPR [4–6], the present study also considers the recently revised ICRU 73 [7] stopping-power data for ions heavier than helium on water. These data replace the ones originally published in ICRU 73 which led to a still ongoing discussion on stopping powers for water targets (see, e.g., [8]) especially in view of recent measurements by Schardt *et al.* [9].

TRS-398 explicitly states that the STPR for water to air, $S_{\text{water/air}}$, should be obtained by averaging over the complete spectra of particles present. And consequently, this requirement was considered to be an important limitation in the case of heavy charged particles, where the determination of all possible particle spectra was assumed to be a considerable undertaking. While this was the case a decade ago and may still be true from the point of view of dose determination for routinely quality assurance nowadays, the determination of complete spectra of particles can be achieved by applying Monte Carlo transportation codes exploiting the now commonly available computer power. These codes are in general valuable in predicting radiation fields of ions in tissues and are in particular useful in hadron therapy for the simulation of ion transport. The most common codes in particle therapy with ions heavier than protons are Geant4 [10], FLUKA [11], MCNPX [12], and SHIELD-HIT [13,14], all taking into account the atomic interaction of the ions with the target medium as well as the nuclear interaction. It is the former interaction which mainly leads to energy loss of the incident ions and therefore the stopping power, while the latter interaction is responsible for fragmentation and therefore for the production of particle spectra.

Initial studies on STPRs relevant for dosimetry in radiation therapy with ions heavier than protons were performed without Monte Carlo calculations ignoring the influence of the secondary particle spectrum (e.g. [15–17] as presented in TRS-398 [2]). Calculations exploiting the capabilities of Monte Carlo codes were performed with SHIELD-HIT but exclusively carbon-ion fields [4–6] were studied. However, the dependence of the STPR on different ion species is of interest since a number of facilities world-wide (e.g., NIRS and HIT) are equipped with radiation fields which cover a broader range of ions than merely protons and carbon ions. Furthermore, it was recently argued that ions heavier than carbon may play an important role in the near future concerning the radiation therapy of radio-resistant tumors [18]. Consequently, a large variety of ion species, namely, H, He, Li, C, N, O, Ne, Si, and Ar are considered here — all accessible either for clinical radiation therapy (up till O and Ne at HIT and NIRS, respectively)

or for in vitro radiobiology experiments.

Another point is noteworthy in a clinical context. Despite their obvious relevance in medical application, so far, STPRs for spread-out Bragg peaks (SOBPs) have been discussed only scarcely in literature. In the work on STPRs for carbon ions by Henkner *et al.* [4], it was stated that — using their preferred set of I -values for water and air — the recommended value 1.13 would lead to an under dosage for a SOBP which is, however, reduced toward the end of the SOBP. And hence, the absorbed dose to water measured for a uniform SOBP with a constant STPR would in reality be inhomogeneous. At the same time, Henkner *et al.* argued that it is not straightforward to correct for this effect, since it may depend on the depth modulation of the SOBP in general, and in particular, in ion beam therapy the applied doses are modulated to account for the variation in the biological effect. Finally, it was outlined in the same reference that a more detailed analysis especially for SOBPs is clearly needed since their statement was only based on the analysis of a single *physically* optimized SOBP using one set of stopping-power data. Consequently, one focus of this work should be a systematic study of the STPR of SOBPs, both *physically* and *biologically* optimized. This may also include SOBPs of different widths and practical ranges and may lead to an analytic expression for STPRs as a function of the residual ion range in the case of SOBPs.

This paper is organized as follows. First, an overview on physics relevant for the STPR is provided including discussions on stopping powers, mean excitation energies, and definitions. Subsequently, the employed methods are discussed and analytic descriptions for the average energy of the primary ions as well as STPRs are proposed. In the next section, the results for pristine as well as SOBPs are presented. The following discussion concentrates on three issues, namely, the influence of the stopping-power data on the STPR, the dependence of the STPR on the ion energy, and STPRs for SOBP.

2. Overview

2.1. Stopping powers

Stopping power is defined as the average energy change dE of a particle per unit length dl in a medium. It is common practice to tabulate *mass stopping powers* [7]

$$\frac{S}{\rho} = -\frac{1}{\rho} \frac{dE}{dl}, \quad (2)$$

which provide the central information about the stopping power but are at the same time independent of a specific media density ρ . At high energies, that is about from 10 MeV/u up to 1 GeV/u,§ the mean energy loss of a charged particle to atomic electrons is well approximated by Bethe's original theory [19,20] which treats the electromagnetic interaction in first-order quantum perturbation theory. At lower energies, however, additional higher-order terms are required in order to reproduce experimental results.

§ The energy regime from 10 MeV/u up to 1 GeV/u, corresponds according to the revised tables for water in ICRU 73 [7], for carbon ions to a range from 0.0427 cm up to 108.6 cm.

The transition from the regime of quantum perturbation theory to the one permitting a classical treatment is described in Bohr's distinguished survey paper [21].

A widespread formulation of Bethe's theory summarizing all terms of the lowest-order stopping number L_0 was proposed by Fano [22]

$$\frac{S}{\rho} = \frac{4\pi e^4}{m_e v^2} \frac{1}{u} \frac{Z}{A} z^2 \left[\ln \frac{2m_e v^2}{I} + \ln \frac{1}{1 - \beta^2} - \beta^2 - \frac{C}{Z} - \frac{\delta}{2} \right], \quad (3)$$

with

$$\frac{4\pi e^4}{m_e v^2} \frac{1}{u} \frac{Z}{A} z^2 = 0.307075 \frac{z^2}{\beta^2} \frac{Z}{A}, \quad (4)$$

in units of MeV cm²/g. In Eq. (3), m_e is the electron mass, e and u are the elemental units of electric charge and atomic mass, respectively, Z and A are the atomic number and the relative atomic mass of the target medium, respectively, v and z are the velocity and the charge of the projectile, and $\beta = v/c$ where c is the velocity of light in vacuum. The mean excitation energy of the target medium is denoted by I , while C/Z and $\delta/2$ are the shell corrections and the density-effect correction^{||}, respectively. The second and third term in the square brackets containing β originate from Bethe's relativistic extension [20] and are often referred to as relativistic corrections. The expression in Eq. (3) is consistent with the description of the stopping-power formula in ICRU report 49 [17] using only the first term L_0 of the stopping number L .[¶]

For low energies the description of the stopping powers becomes more complicated and higher-order terms of the stopping number L have to be taken into account in order to correct for a number of different effects, like the Barkas and the Bloch correction, L_1 and L_2 , respectively. An effective description of the stopping power for the energy regime below the stopping-power maximum was provided by Lindhard and Scharff [23]. The approach by Lindhard and Scharff assumes for energies below the stopping-power maximum a rise of the stopping power which is linear in the square root of the energy.

2.2. Mean excitation energy

The mean excitation energy, I , is a quantity, which is independent of the properties of the projectile, and depends only on the properties of the medium. It enters logarithmically in the stopping formula Eq. (3), and is responsible for most of the stopping-power dependence of the target material. According to Eq. (3) a larger I -value results in a smaller stopping power and consequently in a larger range of an ion in the medium.

First, I -values are obtained from experimental data by comparing to a stopping formula [17,24,25]. This method has the disadvantage that a number of corrections in the

^{||} The Bethe stopping-power formula [19] implies that the projectile is much faster than the bound target electrons. The shell corrections account for deviations from this assumption for low projectile energies. The density-effect correction takes into account the reduction of the stopping power resulting from the polarization of the medium by the projectile.

[¶] The usage of the term $W_m = 2m_e v^2 / (1 - \beta^2)$ as an approximation to the largest possible energy loss in a single collision with a free electron in Eq. (3) is well justified for the energy ranges of the ions discussed here [17].

applied stopping formula might not be known independently with the desired accuracy. Consequently, the I -value becomes to a certain degree a fitting parameter rather than an absolute target-specific quantity. Second, the mean excitation energy I can in principle be obtained theoretically from the optical dipole oscillator strength for gases or the dielectric response function for condensed materials [7]. However, the corresponding advanced electron-structure calculations are demanding and may therefore require the introduction of approximations which in turn lead to inaccuracies with respect to the mean excitation energy I .

The I -values in the ICRU report 49 [17] for protons and alpha particles are retained from ICRU report 37 for electrons [24] where they were mainly taken from measurements. In ICRU report 73 [7], however, the I -values are mostly determined theoretically. As a result different I -values for the same material are recommended in ICRU reports 37 and 49 on the one hand and report 73 on the other hand. Obviously, this is inconsistent, since an I -value should only depend on the target material but not on the projectile. The existing differences show that the current accuracy of the employed methods to determine stopping-power data have still to be improved in order to provide a consistent target description.

While stopping in elemental materials has been the dominating object of both experimental and theoretical studies, in numerous application like, e.g., particle therapy the prime interest concentrates on stopping in compounds. However, in the case of compounds accurate experimental as well theoretical data are often missing from which I -values could be extracted. A common reference standard is *Bragg's additivity rule* [26], which assumes that the stopping cross section of each species is unaffected by the state of aggregation [7] and that the mass stopping power for a compound can be approximated by a linear combination of the stopping powers for the atomic constituents:

$$\frac{S}{\rho} = \sum_{\nu} w_{\nu} \left(\frac{S}{\rho} \right)_{\nu} , \quad (5)$$

where w_{ν} is the fraction by weight and $(S/\rho)_{\nu}$ the mass stopping power of the ν 'th constituent. In view of the stopping formula in Eq. (3) this linear additivity corresponds to an average Z/A ratio,

$$\left\langle \frac{Z}{A} \right\rangle = \sum_{\nu} w_{\nu} \left(\frac{Z_{\nu}}{A_{\nu}} \right) , \quad (6)$$

and to a relation for the mean excitation energy,

$$\ln I = \left[\sum_{\nu} w_{\nu} \left(\frac{Z_{\nu}}{A_{\nu}} \right) \ln I_{\nu} \right] / \left\langle \frac{Z}{A} \right\rangle , \quad (7)$$

of a compound.

In contrast, ICRU recommends another set of I -values for the atomic constituents of a compound — distinguishing also between gaseous and non-gaseous compounds, e.g., Table 2.11 in ICRU 49 [17] — which differs from the set of I -values for elements. The latter approach for compounds — also using Eq. (7) — leads in general to better

agreement with experiment though, it differs from the original Bragg additivity for pure elements described before. However, it is only the original Bragg additivity scheme which allows for the addition of stopping-power data for elements directly taken from tables or measurements for these elements.

2.3. Stopping-power ratio

The stopping-power ratio $S_{a/b}$ between medium a and medium b is, in accordance with IAEA TRS-398⁺ [2], given as a particle fluence weighted average over all primary and secondary particles. It is determined by calculating the dose ratio via track-length fluence $\Phi_{a,i}(E)$ of particle i in medium a as function of particle energy E and according mass stopping power $S_i(E)/\rho$

$$S_{a/b} = \frac{\sum_i \int_{E_{\min}}^{\infty} \Phi_{a,i}(E) (S_i(E)/\rho)_a dE}{\sum_i \int_{E_{\min}}^{\infty} \Phi_{a,i}(E) (S_i(E)/\rho)_b dE} \quad (8)$$

In Eq. (8) numerator and denominator are equal except for that the mass stopping power of medium a enters in the numerator and of medium b in the denominator.

In order to obtain accurate track-length fluences for primary and all secondary particles it is necessary to use Monte Carlo particle-transport calculations which take into account all relevant physical effects like, e.g., nuclear reactions. However, the according codes often use a transport cutoff > 0 . On the other hand, an energy cutoff $E_{\min} > 0$ may originate from the chamber geometry. The contribution of “track-ends” to the total dose deposition and to the corresponding STPR was studied in [27]. There it was concluded that they are not of relevance for light-ion dosimetry which is in contrast to electrons, where the contribution to the total deposited dose can be between 6% and 8% [24]. In a recent review article [28] the impact of electrons in fast ion-atom collisions with respect to hadron therapy has been discussed in more detail.

In contrast to the correct definition for the STPR of an ion field in Eq. (8), the *ratio of stopping powers* for media a and b for one particle of energy E ,

$$\frac{(S(E)/\rho)_a}{(S(E)/\rho)_b} = \frac{\langle \frac{Z}{A} \rangle_a \ln[2m_e v^2/I_a]}{\langle \frac{Z}{A} \rangle_b \ln[2m_e v^2/I_b]}, \quad (9)$$

has often been considered, e.g. [2, 4, 5], as an approximation to the STPR. The right hand side of Eq. (9) $(S(E)/\rho)$ is expressed by Bethe’s stopping formula, that is as in Eq. (3) but omitting corrections. In the case that it is meaningful to approximate the particle spectra at a depth d by a mono energetic particle the ratio of stopping-powers in Eq. (9) may indeed be used as approximation of the STPR. However, the ratio in Eq. (9) considers only one particle species and is a function of its *energy* E in contrast to the STPR in Eq. (8) which takes the whole energy spectra of all particles into account

⁺ In IAEA TRS-398 only the STPR for water-to-air is explicitly defined, i.e., a =water and b =air. However, this definition is also useful for other media combinations.

and has a *spatial* dependence. For the special case of the ratio of stopping powers for water and air, Eq. (9) reads

$$S_{\text{water/air}}(E) = \frac{(S(E)/\rho)_{\text{water}}}{(S(E)/\rho)_{\text{air}}} = 1.11195 \frac{\ln[2m_e v^2/I_{\text{water}}]}{\ln[2m_e v^2/I_{\text{air}}]}. \quad (10)$$

3. Methods

For all our calculations we used the Monte Carlo particle transport code SHIELD-HIT [6, 14], based upon the most recent version SHIELD-HIT07. New functionalities were added to SHIELD-HIT07 [29], most relevant here the possibility of directly scoring the STPR of any media, which will be described in more detail in section 3.2. Apart from this, raster scan files generated by the treatment planning software TRiP [30, 31], can now be read by SHIELD-HIT in order to recalculate SOBPs. A ripple filter implementation based on the design described by Weber *et al.* [32] is added to SHIELD-HIT in a similar way as specified by Bassler *et al.* in [33], in order to produce flat SOBPs.

The practical range, R_p , is defined for protons as the depth at which the absorbed dose beyond the Bragg peak or SOBP falls to 10% of its maximum value. However, for ions heavier than protons this definition of R_p is not applicable in general due to the pronounced dose tail of secondary particles. Therefore, the depth at which the absorbed dose beyond the Bragg peak or SOBP falls to 50% of its maximum value is proposed and used in the following for ions heavier than hydrogen, i.e., $z > 1$. The residual range R_{res} at a measurement depth d is then defined as

$$R_{\text{res}} = R_p - d \quad (11)$$

where d is the depth of measurement. Furthermore, the measurement depth d_{ref} is defined to be at the middle of the SOBP in accordance with TRS-398 [2].

In this study we present calculations from four single field carbon ion SOBPs, listed in table 1. Here the width of the SOBP is defined as usual by the width in which the dose is above 95% percent [2]. The position of the SOBP always refers to the center of the SOBP. All SOBPs are 3-dimensional dose cubes with equal side lengths and the SOBP optimization is realized with TRiP. The resulting raster-scan file describes the needed amount of particles for each raster point and for each energy slice. This file provides the necessary input for SHIELD-HIT to generate the radiation field which results in the SOBP for the calculation of the STPR along the center axis of the beam.

3.1. Stopping powers in SHIELD-HIT

In the current implementation of SHIELD-HIT the compilation of required stopping-power data can be done in two ways which can be chosen independently for each target medium. First, an arbitrary stopping-power table may be read in as a formatted text file. This allows for the use of, in principle, any stopping data which can be provided in electronic form including, e.g., tabulated data recommended by ICRU reports but

also other common sources of stopping power data like PSTAR [35], ASTAR [35], and MSTAR [34] for ions of hydrogen, helium and lithium to argon, respectively. PSTAR, ASTAR and MSTAR are now accessible from a common open source library *libdedx* [36,37] which is available online and is also applied here. Second, stopping-power data can be calculated internally by SHIELD-HIT using a modified Bethe formula at high energies and a Lindhard-Scharff description [23] at low energies for any kind of material composition using the corresponding material-specific values for I , Z , and A as discussed before in Secs. 2.1 and 2.2.

The Bethe formula used in SHIELD-HIT is similar to the formulation in Eq. (3). But, so far no shell corrections C/Z have been considered. These are known to be most relevant for low energies where, however, the Lindhard-Scharff description is used

Table 1. Specifications of spread out Bragg peaks (SOBPs) for carbon ions in water used in this work. Given are the width along the beam axis, the practical range R_p , and whether the SOBP is optimized for a homogeneous physical dose or biological effective dose. The optimization of the SOBPs was performed by the program TRiP.

SOBP	Width (mm)	R_p (mm)	Optimization
<i>a</i>	50	220	physical
<i>b</i>	80	168	physical
<i>c</i>	50	150	physical
<i>d</i>	100	153	biological

Table 2. Specifications for 6 sets of stopping-power data used in this work. For each set the corresponding I -values for water and air in eV are specified together with the range of ions for which these data are used. The stopping-power data for the first three sets are determined internally by SHIELD-HIT as described in Sec. 3.1 while those of sets 4 to 6 are read in as tables in text format.

SHIELD-HIT uses I -value with stopping-power formula					
Set #	I_{water}	I_{air}	z -range	Source	Comments
1	78	82.8	$z \geq 1$	ICRU 73 [7]	using erratum
2	75	85.7	$z \geq 1$	ICRU 49 [17]	
3	80.8	85.7	$z \geq 1$	Henkner [4]	
SHIELD-HIT reads in tabulated stopping-power data					
Set #	I_{water}	I_{air}	z -range	Source	Comments
4	78	82.8	$z > 2$	ICRU 73 [7]	using erratum
	75	85.7	$z \leq 2$	ICRU 49 [17]	
5	67.2	82.8	$z > 2$	ICRU 73 [7]	without erratum
	75	85.7	$z \leq 2$	ICRU 49 [17]	
6	75	85.7	$z = 1$	ICRU 49 [17]	
			$z > 1$	MSTAR [34]	scaling ICRU 49

instead in SHIELD-HIT. Furthermore, it was demonstrated that for low energies (about 1 MeV/u) the accuracy of stopping-power data is insignificant for particle therapy [38]. The same argument holds for the higher-order term L_1 , often referred to as Barkas term, which corrects for differences in the stopping power between charges with the same absolute value but opposite sign which is relevant for energies around the stopping-power maximum only. Additionally, the Bethe formula is modified in order to allow for electron capture, becoming significant at low energies, by using an effective energy-dependent scaling of the projectile charge z which was proposed by Hubert *et al.* [39]. Currently, relativistic corrections recently proposed by Lindhard and Sørensen [40] are still missing in SHIELD-HIT. Their importance increases especially for heavy ions with large nuclei which cannot be approximated as point-like particles. Although their relevance for the accuracy of particle therapy should explicitly be studied no significant impact has been expected so far.

Due to existing inconsistencies in the stopping-power data recommended by ICRU — as discussed before in Sec. 2.2 — different sets of stopping powers are used in this work, all listed in Table 2. Thereby, sets 1 and 2 as well as sets 4 and 5 are directly related to ICRU reports. Sets 1 and 2 try to describe the target media consistently with only one I -value for ions with $z \leq 2$ as well as for $z > 2$. Set 1 uses only the I -values from ICRU report 73 (the revised value for water, $I_{\text{water}} = 78$ eV, is given in the erratum to ICRU 73) while only I -values from ICRU 49 are used in set 2. The stopping power is then determined by applying SHIELD-HIT's internal routine with the corresponding I -values. Note, the recently revised data from ICRU 73 were not employed by Henkner *et al.* [4].

Sets 4 and 5, on the other hand, directly use the tables provided by ICRU reports 49 and 73 for ions with $z \leq 2$ and $z > 2$, respectively, which are just read as input by SHIELD-HIT. While set 4 uses the recently revised stopping-power data for heavy-ions on water, set 5 uses, for comparison to older studies of the STPR, the water data as originally published in ICRU 73. In addition to the discussed sets including only stopping-power data recommended by ICRU two further sets are employed, i.e., set 3 and set 6. The I -values of set 3 were preferably used by Henkner *et al.* in their study on STPRs [4] while set 6 uses the frequently employed MSTAR stopping-power tables [34]. MSTAR provides stopping-power data for heavy ions by scaling data for alpha particles using basically the results of ASTAR [35] for helium ions. This leads to a more consistent description of the target properties in comparison to the combined use of tables provided by ICRU reports 49 and 73.

3.2. Scoring in SHIELD-HIT and STPR

STPRs have already been obtained with SHIELD-HIT before as described in [4, 6]. However, a number of conceptual improvements have been implemented [41] in the course of this work. Only these are discussed in the following. The scoring in SHIELD-HIT is performed with a recently developed routine [41]. Thereby, the concept of virtual

scoring has been introduced which now allows for an arbitrary spatial arrangement of detector bins. It is therefore independent of physical geometries and there is no need for introducing additional boundaries.

In contrast to the earlier work [4, 6], the STPRs are now determined *on-line*, that is, during the transport of the particles. An on-line calculation has the advantage that possible influence on the result due to the number and size of the energy scoring and energy spacing is avoided. Additionally, higher accuracy in scoring of tracks-ends can be achieved in principle.

The detector for the STPR resembles Eq. (8) and is implemented in the following way. When a particle traverses a bin of the STPR detector its track-length fluence within the bin is scored and directly multiplied with the *mass stopping power* of medium *a* in which the particle moves for the energy $(E_{\text{in}} + E_{\text{out}})/2$. E_{in} and E_{out} are the energies of the particle when it enters and leaves the bin, respectively. Additionally, the *same* track-length fluence is multiplied with the mass stopping power of the same particle but for a different medium *b*. Both quantities are summed up individually for all particles passing the bin. After a full Monte Carlo transport simulation the two sums are divided yielding the STPR for this bin.

In this work a transport cutoff of 0.025 MeV/u is used by SHIELD-HIT which means that all particle tracks end once the particle energy becomes smaller.* Consequently, the lower limit for the integration in Eq. (8) is given by $E_{\text{min}} = 0.025$ MeV/u which has an influence on the STPR of less than 0.00015% [4]. Recently, it has been discussed to extend SHIELD-HIT in a way that also electron tracks are considered in detail [28]. This would finally allow for studies of the microscopic energy distribution in the target medium.

3.3. Average ion energy

The stopping-power formula as presented in Eq. (3) for a specified combination of projectile and target is primarily a function of the projectile's kinetic energy which decreases during the passage through the target medium due to the energy loss. In order to determine the average energy of the projectiles as a function of depth a full simulation of the particle transport has to be performed. This comprises the slowing down caused by all relevant energy-loss mechanisms including elastic as well as inelastic interactions. Thereby, inelastic nuclear reactions produce a spectrum of particles with each particle having an individual energy distribution which is furthermore a function of the position in the medium.

In view of the number of physical processes which all together determine the average kinetic energy of the particles it is highly desirable to have a simple, though approximate, analytical expression for the average energy of the primary particles as function of penetration depth *d*. We start with the Bethe formula, but employ for a while the

* This is consistent with ICRU 73 [7] where the range tables for liquid water show the average path length travelled for slowing-down from initial energy *E* to $E_0 = 0.025$ MeV/u.

assumption that the expression in the square brackets of Eq. (3) is independent of energy. Then the differential equation for the energy can easily be solved. Hence, a preliminary approximation to the energy as function of depth d for an ion with an initial energy E_0 can analytically be expressed,

$$E(d; E_0, R_p) \approx E_0 \left(\frac{R_p - d}{R_p} \right)^{1/2}, \quad (12)$$

where R_p is the practical range. The practical range depends in general on the ion species, its initial energy E_0 , and the target material. For energies relevant in particle therapy R_p can often be approximated using the continuous slowing down approximation (CSDA).

In order to account for the correct energy dependence of all terms of the Bethe formula the preliminary approximation in Eq. (12) might further be scaled with an additional d -dependent factor which yields the relation

$$E(d; E_0, R_p) \approx E_{\text{app}}(d; E_0, R_p) = E_0 \left(\frac{R_p - d}{R_p} \right)^{1/2} \left(\frac{R_p^2 - qd^2}{R_p^2} \right) \quad (13)$$

with a parameter q which is not fixed and may take values in between $q = 0.2$ and $q = 0.3$. The choice of q depends very weakly on E_0 and in general larger q are better suited for larger E_0

3.4. Analytic expression for STPR

In order to derive an analytic, though approximate, expression of the STPR as a function of d for two media a and b , the approximation to the average energy proposed in Eq. (13) can be used together with the ratio of stopping powers given in Eq. (9). Utilizing the non-relativistic relation $v^2 = 2E/m_p$ between the particle velocity v and its kinetic energy E , where m_p is the proton mass and approximating E with $E_{\text{app}}(d; E_0, R_p)$ according to Eq. (13), one obtains the expression

$$\tilde{S}_{(a/b)}(d) = \frac{\langle \frac{Z}{A} \rangle_a}{\langle \frac{Z}{A} \rangle_b} \frac{\ln[E_0/I_a] + C(d)}{\ln[E_0/I_b] + C(d)} \quad (14)$$

where

$$C(d) = \ln[E_{\text{app}}(d)/E_0] - 6.8223 \quad (15)$$

$$= \frac{1}{2} \ln \left[\frac{R_p - d}{R_p} \right] + \ln \left[\frac{R_p^2 - qd^2}{R_p^2} \right] - 6.8223 \quad (16)$$

and $\ln[2m_e/m_p] \approx -6.8223$ have been used. Similar as in Eq. (8) the numerator and denominator in Eq. (14) equal except for that they differ in the I -values and the $\langle Z/A \rangle$ ratios. For energies relevant for particle therapy it can be expected that the magnitude of the STPR in the whole plateau region is mostly determined by the ratio of $\langle Z/A \rangle$ for media a and b since E_0/I , on the other hand, is usually of the order of 10^6 and the difference of $\ln[E_0/I]$ for media a and b is therefore rather small. It should be mentioned that in order to keep the expression for $\tilde{S}_{(a/b)}$ as simple as possible its derivation has

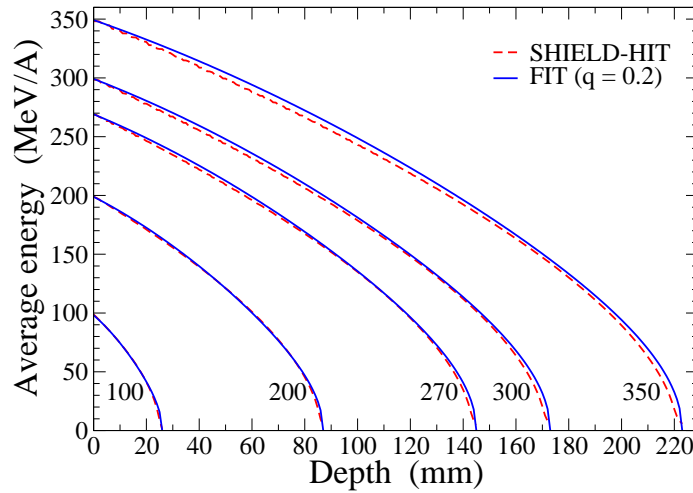


Figure 1. Average energy of carbon ions as a function of depth in water for carbon ion beams with different initial energies from 100 MeV/u to 350 MeV/u. Only set 1 of Table 2 is used. These data are compared to the fit in Eq. (13) using $q = 0.2$.

been performed without relativistic kinematics which are in principal of relevance for the highest energies used in particle therapy. Finally, the expression in Eq. (14) should explicitly be formulated for the STPR for water to air,

$$\tilde{S}_{(\text{water/air})}(d) = 1.11195 \frac{\ln[E_0/I_{\text{water}}] + C(d)}{\ln[E_0/I_{\text{air}}] + C(d)}, \quad (17)$$

being the most relevant case for dosimetry in particle therapy.

4. Results

In the following only results for ion beams in water are considered, and STPRs are presented exclusively for water to air.

4.1. Pristine Bragg peaks

The average energy of carbon ions as a function of depth in water extracted from calculations with SHIELD-HIT is shown in Fig. 1. Different initial energies relevant for particle therapy with carbon ions are considered ranging from 100 MeV/u up to 350 MeV/u. An I -value of 78 eV for water as recommended by ICRU report 73, set 1 of Table 2, is used. The analytic expression for the average energy of primary ions as function of the initial energy and depth in water proposed in Eq. (13) using $q = 0.2$ compares favorably with the data obtained with SHIELD-HIT. The largest differences can be observed around a depth of 1/3 of the total range and at the end of the track where a strong deceleration of the primary ions occurs. Clearly, it is the latter effect at the end of the track which causes the Bragg peak in a depth-dose distribution.

The effect of varying the stopping-power data on the STPR is demonstrated in Fig. 2(a) for a 270 MeV/u carbon pencil beam. In the plateau region, the deviations for all

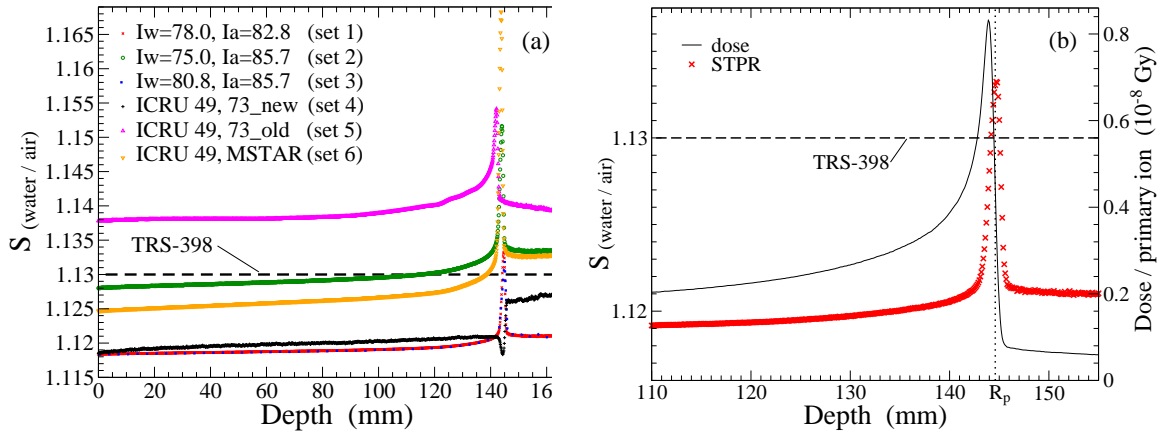


Figure 2. Stopping-power ratio for water to air $S_{\text{water/air}}$ for a 270 MeV/u carbon ion beam as a function of the depth in water. (a) Shown are sets 1–6 of Table 2 and the value 1.13 as recommended in TRS-398 by the IAEA [2]. (b) Only set 1. STPR and according depth-dose distribution per incident ion.

sets 1 to 6 of Table 2 from the value 1.13 recommended by the IAEA in the TRS-398 [2] is within 1% and set 2 differs the least. This is consistent since the recommendation in TRS-398 is based on the stopping data and I -values, set 2, provided by ICRU report 49. However, except for the recommended value 1.13, none of the calculated STPR curves is constant. The relative increase in the plateau region up to a depth of 130 mm is moderate and of the order of approximately 0.2% to 0.3%. For all sets of stopping powers, except of set 4, an increase of the STPR can be observed in the vicinity of the Bragg peak. Set 4 on the other hand shows a dip.

Although the I -values of set 1 and set 3 — the latter was used in [4] — differ notably, are the two STPR curve in Fig. 2(a) virtually on top of each other. This can be explained by the similar differences of the I -values for water and air which are 4.8 eV and 4.9 eV for set 1 and set 3, respectively. On the other hand, no unphysical minimum of the STPR in the plateau region for stopping-power data from ICRU, set 5, as was observed in [4], results from the present calculations. Note, the position of the Bragg peak is (only) influenced by the choice of stopping-power data for water.

A comparison between the calculated STPR for water to air of 270 MeV/u carbon ions as a function of depth in water and the corresponding depth-dose distribution is shown in Fig. 2(b) for set 1 of Table 2. The maximum of the STPR almost coincides with the practical range $R_p = 144.6$ mm and therefore appears to be at a larger depth than the dose maximum. The width of the STPR peak is considerably smaller than that of the dose curve, while the determined height of the STPR depends to some extent on the finite spatial resolution along the beam axis which leads to a spatial averaging.

Figure 3 shows STPRs for carbon ion beams with different energies as a function of the residual range in water R_{res} , where the latter is defined according to Eq. (11). Using this representation the STPR curves are almost identical in the plateau region. Around and beyond the Bragg peak the curves are still alike, though in this region, lower initial

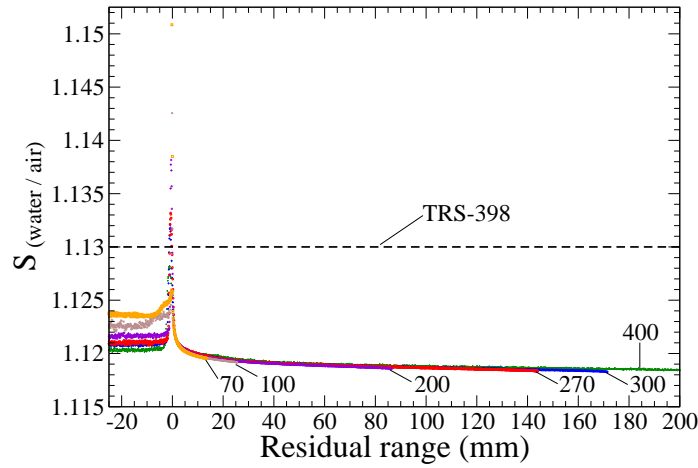


Figure 3. Stopping-power ratio for water to air $S_{\text{water/air}}$ for carbon ion beams as a function of R_{res} in water. Only set 1 from Table 2 is used. Different initial ion energies ranging from 70 MeV/u to 400 MeV/u are compared.

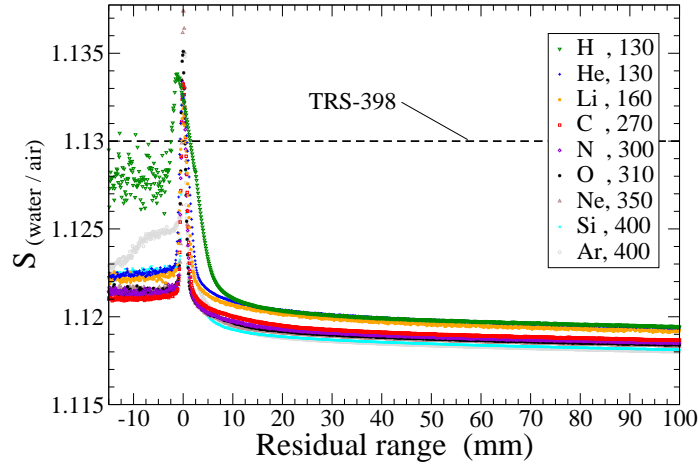


Figure 4. Stopping-power ratio for water to air $S_{\text{water/air}}$ as a function of R_{res} in water for different ion beams relevant for particle therapy: H, He, Li, C, N, O, Ne, Si, and Ar. Different ion beam energies ranging from 130 MeV/u to 400 MeV/u have been chosen in order to achieve comparable penetration depths. Only set 1 of Table 2 is used.

energies lead in general to higher STPRs values.

In Fig. 4 STPRs as a function of the residual range R_{res} in water are presented for different ion beams relevant for particle therapy: H, He, Li, C, N, O, Ne, Si, and Ar. Different beam energies for the individual ions have been chosen, ranging from 130 MeV/u to 400 MeV/u, in order to achieve comparable penetration depths. For a consistent comparison only stopping-data set 1 of Table 2 is used. In the plateau region the STPRs for all the different ion beams show the same qualitative behavior already discussed for carbon ions in Figs. 2 and 3. In general, a decrease of the STPR at a given R_{res} can be observed with an increase of the atomic number z of the ion, while the decrease becomes smaller for larger z . An exception are H and He ions for which

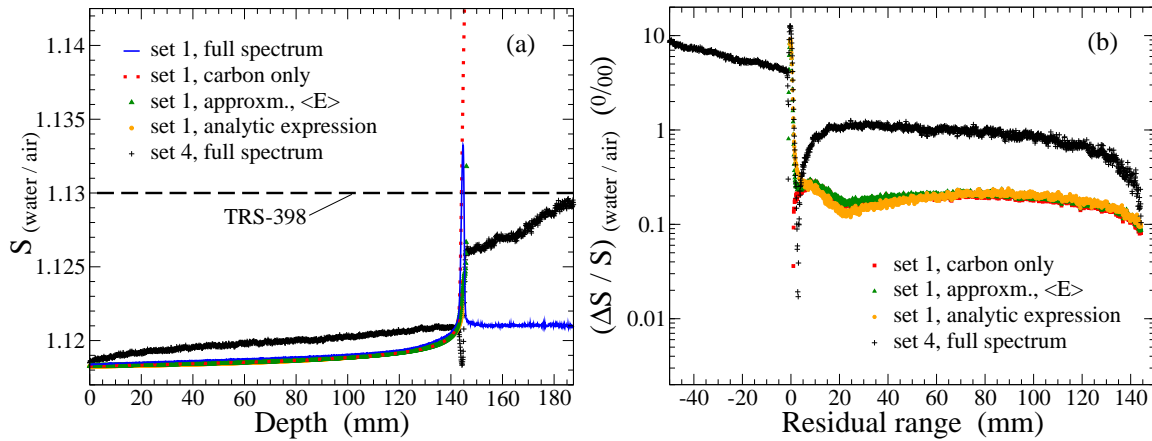


Figure 5. Stopping-power ratio for water to air $S_{\text{water/air}}$ for a 270 MeV/u carbon ion beam in water. Only sets 1 and 4 of Table 2 are used. The STPR for the full particle spectrum using set 1 is compared to the STPRs (i) calculated only for carbon ions, (ii) determined with the approximation in Eq. (10) using the average energy $\langle E \rangle$ of the carbon ions, (iii) using the analytic expression proposed in Eq. (17), and (iv) the STPR for the full particle spectrum using set 4. (a) Total $S_{\text{water/air}}$. (b) Relative difference between the STPR for the full particle spectrum using set 1 and the other four STPRs as shown in (a).

the STPR curves can be considered to be on top of each other. The relative difference of STPRs between the lightest and heaviest ion $z = 1$ and $z = 18$, respectively, is rather constantly of the order of 0.15%. Around and beyond the Bragg peak, the STPR — although depending quantitatively also on the energy of the ion beam, as observed in Fig. 3 — seems to be larger for ions with larger z . While the STPR for H ions is nearly identical to that for He ions in the plateau region, differences to all other ions with $z > 1$ are obvious around and beyond the STPR maximum. However, as discussed in Sec. 3, the definition of the practical range R_p for protons differs from that used for ions with $z > 1$ which influences — according to Eq. (11) — also the residual range R_{res} .

The dependence of the STPR on the way how it is determined is exemplarily shown in Fig. 5 considering $S_{\text{water/air}}$ for a 270 MeV/u carbon ion beam in water. For set 1, the STPR determined according to Eq. (8) using the *full* particle spectrum calculated with SHIELD-HIT — as presented in Fig. 2 — is compared to three approximations of the STPR: (i) STPR calculated only for carbon ions ignoring the influence of produced fragments, (ii) STPR determined with the approximation in Eq. (10) using the average energy $\langle E \rangle$ of carbon ions as scored by SHIELD-HIT in order to estimate v^2 , and (iii) STPR determined with the analytic approximation in Eq. (17). Additionally, the STPR determined with the *full* particle spectrum is shown for set 4.

Especially in the plateau region, the absolute difference between these curves is small as can be seen in Fig. 5(a). Therefore, Fig. 5(b) shows the relative difference $|S^{\text{full}} - S^{\text{appr}}| / S^{\text{full}}$ between the STPR for the *full* particle spectrum using set 1 and the other four STPRs presented in (a). The three approximations reproduce the STPR determined according to Eq. (8) with the full spectrum within less than 0.03% in the

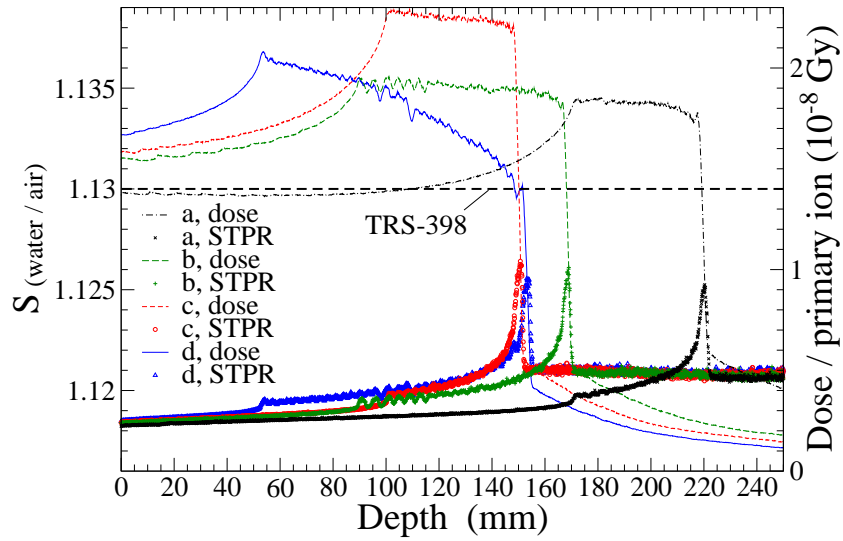


Figure 6. Dose distributions (lines) of four SOBPs for carbon ions as specified in Table 1 together with the according STPRs $S_{\text{water/air}}$ for water to air (symbols) as a function of depth in water. Only set 1 of Table 2 is used.

whole plateau region. Around the STPR maximum the difference can be larger than 1%. In comparison, the STPR calculated with set 4 using the *full* particle spectrum also deviates by the same order of magnitude around and beyond the maximum. In the plateau region the difference is moderate and of the order of 0.1 %.

4.2. Spread-out Bragg peaks

Four different SOBPs obtained with carbon ion fields are considered in Fig. 6 and their properties are listed in Table 1. Figure 6 displays the depth-dose distributions (lines) and the corresponding STPRs (symbols) of the SOBPs *a* to *d* calculated with set 1. At the depth where the dose reaches the peak height the STPRs of all four SOBPs show a significant increase. Towards the distal end of the SOBP the STPRs reveal an exponential increase. At the practical range R_p a sharp fall off of the STPR occurs which finally results for depths larger than R_p in a constant STPR being the same for all four SOBPs. Note, this qualitative description is valid for all SOBPs *a* to *d* and is therefore independent of the specific form of the SOBP or whether it is physically or biologically optimized.

The STPRs of all four SOBPs are compared in Fig. 7(a) as a function of R_{res} . The SOBPs *a* and *c* share the same width and only differ in the depth of the SOBP region, that is R_p . Therefore, their STPRs as a function of R_{res} are nearly identical. The STPR curves for *b* and *d* show a very similar behavior which is extended to 80 and 100 mm, respectively, according to their larger width of the SOBP region. As a result, a simple fit, also shown in Fig. 7(a), may be proposed

$$S_{\text{water/air}}(d) = \alpha + \beta \exp[\gamma(R_p - d)] + \delta(R_p - d) \quad (18)$$

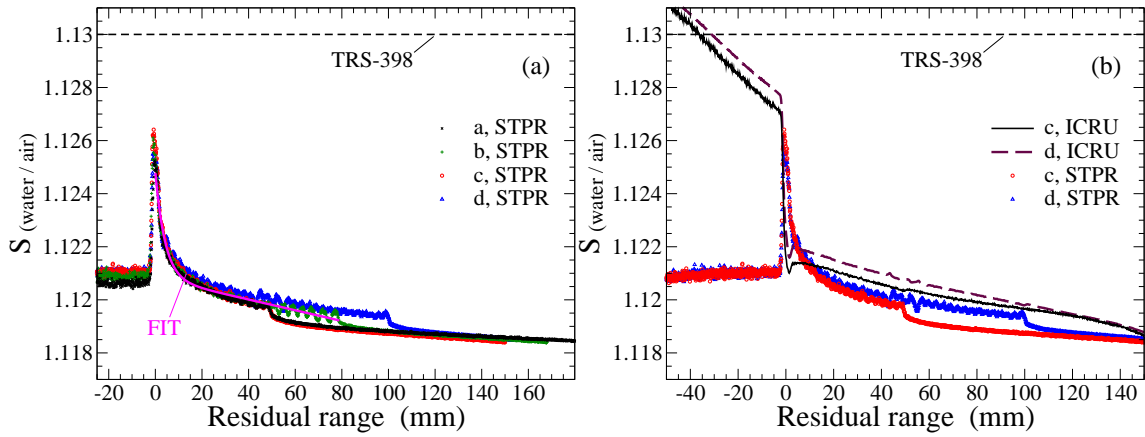


Figure 7. (a) The same as Fig. 6 but as a function of the residual range R_{res} in water. Also shown is a simple fit for set 1 proposed in Eq. (18). (b) The STPRs of the SOBPs c and d of Table 1 are compared using set 1 and set 4 of Table 2.

which approximates the STPR within the SOBP region. The relation between d and the residual range R_{res} is given in Eq. (11) and the values for the constants are

$$\alpha = 1.12082, \quad \beta = 0.004, \quad \gamma = -0.241, \quad \text{and} \quad \delta = -2.0216\text{E-}05.$$

Outside the SOBP region the STPR might be approximated in a similar way as it is done for pristine peaks. Obviously, it is straightforward to use the depth d directly in the fit formula in Eq. (18) by applying the simple relation in Eq. (11) between d and R_{res} . It should be mentioned that for SOBP b a number of ripples in the STPR can be observed in the proximal SOBP region. They originate from the optimization program TRiP which assumes treatment at the SIS accelerator at Gesellschaft at Schwerionenforschung (GSI), Darmstadt, Germany which provides finite energy steps resulting in the observed ripples in the lowest energy part of the depth-dose distribution as well as in the STPR.

Figure 7(b) compares the STPRs for SOBPs c and d using set 1 — as before in Fig. 7(a) — and set 4 of Table 2. While the quantitative difference between the curves for set 1 and set 4 is small for depths less than R_p , the discrepancy between these STPR curves is mainly qualitative in this range. The different behavior of the STPR beyond the SOBP obtained with set 1 and set 4 resembles very much the STPRs beyond the Bragg peak for a pristine peak with set 1 and set 4 shown in Fig. 5.

The calculated STPR and dose transverse to the beam axis at the reference depth $d_{\text{ref}} = 150$ mm — defined in TRS-398 as the middle of the SOBP — is displayed in Fig. 8 for the SOBP c using set 1. The STPR is perfectly constant within the full extension of the SOBP transverse to the beam axis. A moderate increase of the STPR occurs outside the SOBP.

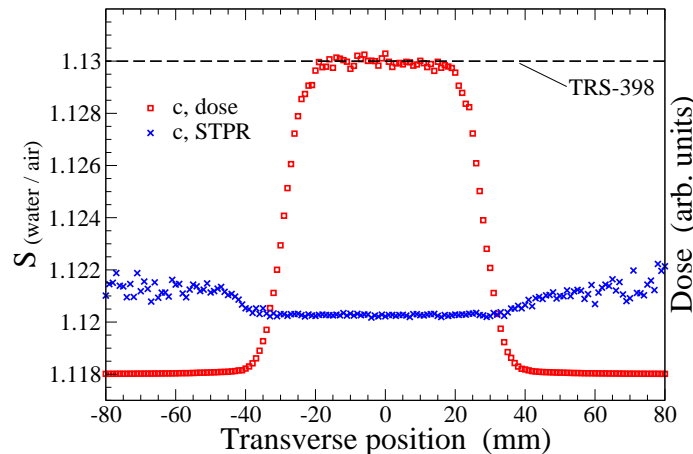


Figure 8. Dose distribution of the SOBP c for carbon ions as specified in Table 1 together with the according STPR $S_{\text{water/air}}$ for water to air as a function of transverse range in water at the $d_{\text{ref}} = 150$ mm. Set 1 of Table 2 is used.

5. Discussion

5.1. Influence of the inconsistency of ICRU stopping-power data on the STPR

It is obvious that the STPR strongly depends on the stopping-power data which are used as an input for its determination. This applies for the value of the STPR as well as the position of the Bragg peak. Therefore, the present work focuses mainly on stopping-power values for water and air which are recommended by ICRU reports. However, even if one tries to follow these recommendations certain inconsistencies still remain and different sets of stopping-power data — as listed in Table 2 — can be deduced. In the case that the tables provided by ICRU are used directly, set 4, the target media water and air possess different physical quantities, e.g. the I -value, depending on whether they interact with protons and helium ions or whether they interact with heavier ions. Another way — being somewhat more consistent from a physical point of view though not explicitly recommended by an ICRU report — is to use the I -values of either ICRU report 49, I_{49} , or 73, I_{73} , together with an appropriate stopping formula for both ions with $z \leq 2$ as well as $z > 2$ which is done in set 2 or set 1, respectively.‡

Figure 2 reveals that the STPR using only I_{49} for all ions, set 2, agrees best with a constant value of 1.13 as recommended in TRS-398. This is not surprising since the TRS-398 builds mainly on the stopping data provided by ICRU 37 and 49 — the I -values used in the latter are directly taken from the former. The STPR obtained by taking into account only the I -values of ICRU 73, set 1, is about 1% smaller than that obtained

‡ A further option is to correct for the I -value in one of the two recommended sets of ICRU tables leading to a more consistent description of the target media. According to Eqs. (3) and (4) this could be done in first order using the term $0.307075 (z^2 Z) / (\beta^2 A) \ln[I_{49}/I_{73}]$ for correcting ICRU report 49 or its negative value for correcting ICRU report 73 [42]. This approach is of course not applicable in the low-energy regime where, on the other hand, the ICRU tables anyhow provide a limited accuracy only. This option has, however, not been pursued in this work

with set 2. On the other hand, the deviations of the STPR using set 1 and tabulated values from ICRU 49 and 73, set 4, is only of the order of 0.1% in the whole plateau region, as can be seen in Fig. 5(b). Though, the use of set 4 leads to a remarkably different behavior of the STPR around and beyond the Bragg peak. Instead of a sharp maximum, observed for all other stopping-power data sets, a minimum occurs. The minimum does not originate from differences in the target descriptions due to the use of ICRU 49 and 73 but is exclusively caused by the low-energy ratio of stopping powers taken from ICRU 73. The steep increase of the STPR curve beyond the minimum for set 4 and its trend towards the values obtained with set 2, on the other hand, clearly reveal the transition from ICRU 73 to 49 — and therefore intrinsically from I_{73} to I_{49} — due to the shift of the particle spectrum towards lighter fragments, i.e., protons and alpha particles beyond the Bragg peak.

The use of the out-dated standard, that is stopping tables from ICRU 49 and 73 *without* the revisions of ICRU 73 for water, set 5, is not advised. Set 5 yields a STPR which is in the plateau region about 1% and 2% larger than the value 1.13 recommended by TRS-398 and the values obtained *with* revisions of ICRU 73 for water, set 4, respectively. It should be mentioned, that the results for set 5 in Fig. 2(a) do not show any unphysical minimum in the plateau region as was observed before in [4, 5]. There, the unphysical structure was attributed to the use of different stopping-power data from ICRU 49 and 73 for different ions. However, in the present work it was possible to reproduce the exact shape of the curve as shown in Fig. 2 of [4] by using only three digits of the stopping-power data of ICRU 49 and 73 instead of the four digits provided by the tables and therefore to contradict the earlier statement. In conclusion, we can state that the reason for the unexpected behavior observed in the corresponding Fig. 2 of [4] is simply due to errors resulting from a too coarse rounding in the applied stopping-power list and are not caused by a combined use of ICRU 49 as well as 73.

5.2. Dependence of the STPR on the average ion energy

One quintessence of this work is that the STPR for a given set of stopping-power data is mostly determined by the average energy of the ions, rather than their initial energy or their charge. This is nicely confirmed in Fig. 3 where it can be seen that the STPRs compared at a given residual range R_{res} are the same for different initial beam energies. Figure 5 shows furthermore that in the plateau and the Bragg-peak region the STPR, obtained according to TRS-398 using the full particle spectrum, can be reproduced if the average energy of the primary ions is known as a function of depth. According to Fig. 5(b) a relative deviation of the order of only 0.02% is achieved if simply the ratio of the two stopping powers for these average energies is taken. Additionally, the average energy of the primary ions as a function of depth can easily be approximated — using Eq. (13) — once their initial energy and total range are known. Consequently, for any given set of stopping data, e.g. tables from ICRU or a set of I -values, a STPR can very easily be approximated with an accuracy much below 0.05%. It is noteworthy, that the

proposed approximative approach is in principle not restricted to a specific combination of target materials, like, e.g., water and air being in the focus of this work. The approach is rather able to provide STPR for any set of stopping-power data if a relation between the average energy and the depth is obtained according to Eq. (13).

This findings lead to two central insights. First, in contrast to the presumption in TRS-398, in the case of pristine peaks the knowledge of the whole particle spectra is not of practical importance for the plateau and Bragg peak region.^{††} The STPR can be simply approximated with a relative deviation much smaller than the accuracy of all currently available stopping-power data. On the other hand, it is obvious that beyond the Bragg peak where practical all primary ions are ceased the secondary particles are of central importance. Second, it is not necessary to study STPRs for all ions independently. The small quantitative differences among the STPRs of the various ions shown in Fig. 4 may be explained best with the different average energies of the ions at a given R_{res} . Additionally, the STPR for all ions can be approximated in the same way as proposed above in Eq. (14). Furthermore, this approximation is in principle not limited to a specific combination of materials like water and air. For example, it can be straightaway used for STPR for water to tissue and air to tissue which would be of interest when comparing dose to medium with dose to water as recently discussed by Paganetti [43].

5.3. STPRs for SOBPs

Clinical applications require a relatively uniform dose to be delivered to the volume to be treated and for this purpose the ion beam has to be spread out both laterally and in depth. With respect to the STPR of SOBPs the gist of this work is that the qualitative behavior of the STPR is hardly dependent on the specific spatial form of the SOBP, its depth in the medium, and whether it is optimized for a homogeneous physical dose or biological effective dose.

This statement is nicely verified in Fig. 7(a) where the STPR is displayed as a function of residual energy for four different SOBPs specified in Table 1. In order to understand the observed uniform behavior of the STPR one has to keep in mind that a SOBP is just a superposition of Bragg peaks of different intensities and energies which is usually constructed from the distal end, i.e. $R_{\text{res}} = 0$, toward the proximal start. Consequently, the properties of the SOBP up till a residual range R_{res} are only very little influenced by the properties of the SOBP for larger R_{res} . It is therefore possible and practical to propose an empirical fit to the STPR for the SOBP region, as it is done in Eq. (18) for carbon ions and set 1, starting from $R_{\text{res}} = 0$ up till the total width of the SOBP.

On the other hand, the qualitative dependence of the STPR on the set of stopping-power data can be seen in Fig. 7(b). As for the pristine peaks discussed before the

^{††}The relevance of the whole particle spectra for determining the STPR increases if for some secondary particles different stopping-power data are employed, e.g. ICRU 73 and 49.

quantitative difference between set 1 and set 4 is of relevance around and beyond the Bragg peak owing to two facts. First, the ICRU 73 tables, set 4, lead to a minimum of the STPR where there is a maximum when the I_{73} values, set 1, are used. Second, the strong increase of the STPR beyond the peak for set 4 stems from the use of ICRU 49 tables for protons and helium which results according to Fig. 2(a) in a STPR of approximately 1.13.

In TRS-398 reference conditions for the determination of absorbed dose for ion beams are specified. The reference depth, i.e. measurement depth d_{ref} , for calibration should be taken at the middle of the SOBP, at the center of the target volume. It can be seen in Fig. 8 that a positioning error of a dosimeter transverse to the beam axis has no relevance on the STPR as long as the position is within the SOBP. This is not surprising since for the same depth the average energy of the ions should be same. A misalignment along the beam axis, on the other hand, may have an influence as seen in Fig. 7. The influence is largest for a SOBP with small width where the gradient of STPR is largest and becomes very small for large widths which therefore might be recommended for accurate dose measurements in a practical quality-assurance setting. The total variation of the STPR along the beam axis observed in Fig. 7(a) for carbon beams using set 1 is of the order of 0.8%.

In this work the STPR for SOBPs is only considered for carbon ion beams. In analogy to the findings for pristine peaks differences can be expected for other ion species but it is not clear if these are also quantitatively of the same order of magnitude. However, a detailed study is beyond the scope of this article and should be addressed in a future work.

6. Conclusions

Calculations of the water-to-air stopping-power ratio (STPR) using the Monte Carlo transport code SHIELD-HIT are performed for ions in a range of $1 \leq z \leq 18$. Besides providing accurate quantitative results a focus is put on a thorough qualitative understanding relevant for particle therapy. The STPR is determined on-line during the calculation as recommended by IAEA in TRS-398 using the track-length fluence spectra of all primary and secondary particles.

STPRs obtained with different sets of stopping-power data recommended by ICRU [7, 17], including the very recently revised data for water, are compared with the value 1.13 recommended in TRS-398 [2] resulting in deviations of the order of 1% in the plateau region. It can be shown that the STPR for a given set of stopping-power data at a residual range R_{res} is mostly determined by the average energy of the ions at that R_{res} , rather than their initial energy or their charge z . A convenient analytical expression for the STPR as a function of depth in water is proposed for the plateau region up to the Bragg peak which deviates in this region by less than 0.03% from the obtained results. For the case of spread-out Bragg peaks (SOBPs) it can be concluded that the qualitative behavior of the STPR is hardly dependent on the specific spatial form of

the SOBP, its depth in the medium, and whether it is optimized for a homogeneous physical dose or biological effective dose. A fit function is provided to approximate the STPR within the SOBP region for carbon ions. Furthermore, the change of the STPR due to the contribution of secondary particles is insignificant for pristine peaks in the plateau region up to the Bragg peak.

Finally, it can be stated that no further theoretical studies of STPRs heading only for higher accuracy are expedient, as long as no consistent set of relevant stopping-power data for all ions is recommended, preferably with smaller error bars.

Acknowledgments

This work is supported by the Danish Cancer Society (<http://www.cancer.dk>), and the Lundbeck Foundation Centre for Interventional Research in Radiation Oncology (<http://www.cirro.dk>).

References

- [1] International Commission on Radiation Units and Measurements. Clinical proton dosimetry part I. - Beam production, beam delivery and measurement of absorbed dose. Technical Report 59, ICRU, 1998.
- [2] International Atomic Energy Agency. Absorbed dose determination in external beam radiotherapy an international code of practice for dosimetry based on standards of absorbed dose to water. Technical Report 398, IAEA, 2000.
- [3] G. H. Hartmann, O. Jäkel, P. Heeg, C. P. Karger, and A. Kriesbach. Determination of water absorbed dose in a carbon ion beam using thimble ionization chambers. *Phys. Med. Biol.*, 44(5):1193, 1999.
- [4] Katrin Henkner, Niels Bassler, Nikolai Sobolevsky, and Oliver Jäkel. Monte carlo simulations on the water-to-air stopping power ratio for carbon ion dosimetry. *Med. Phys.*, 36:1230, 2009.
- [5] Helmut Paul, Oksana Geithner, and Oliver Jäkel. The influence of stopping powers upon dosimetry for radiation therapy with energetic ions. volume 52 of *Advances in Quantum Chemistry*, pages 289 – 306. Academic Press, 2007.
- [6] O. Geithner, P. Andreo, N. Sobolevsky, G. Hartmann, and O. Jäkel. Calculation of stopping power ratios for carbon ion dosimetry. *Phys. Med. Biol.*, 51:2279–2292, 2006.
- [7] ICRU Report 73. Stopping of ions heavier than helium. *J. ICRU*, 5:1, 2005.
- [8] Helmut Paul. Recent results in stopping power for positive ions, and some critical comments. *Nucl. Instrum. Methods Phys. Res. B*, In Press, Accepted Manuscript:–, 2010.
- [9] D. Schardt, P. Steidl, M. Krämer, U. Weber, K. Parodi, and S. Brons. Precision Bragg-curve measurements for light-ion beams in water. GSI Scientific Report 2007 2008-1. 373, GSI, 2008. Available from: <http://www.gsi.de/informationen/wti/library/scientificreport2007/PAPERS/RADIATION-BIOPHYSICS-19.pdf>.
- [10] S. Agostinelli et al. Geant4 - a simulation toolkit. *Nucl. Instrum. Methods Phys. Res. A*, 506(3):250–303, 2003.
- [11] A. Fassò, A. Ferrari, J. Ranft, and P. R. Sala. FLUKA: a multi-particle transport code. CERN-2005-10, INFN/TC_05/11, SLAC-R-773, 2005.
- [12] D. B. Pelowitz. *MCNPX users manual*. Los Alamos National Laboratory, 2005. [Online] Available: <http://mcnpx.lanl.gov>.

- [13] A. V. Dementyev and N. M. Sobolevsky. SHIELD — universal Monte Carlo hadron transport code: scope and applications. *Radiat. Meas.*, 30(5):553–557, 1999.
- [14] Irena Gudowska, Nikolai Sobolevsky, Pedro Andreo, Dževad Belkić, and Anders Brahme. Ion beam transport in tissue-like media using the monte carlo code SHIELD-HIT. *Phys. Med. Biol.*, 49:1933–1958, 2004.
- [15] M. H. Salamon. Range-Energy Program for relativistic heavy ions in the region $1 < E < 3000$ MeV/amu. LBL Report LBL-10446, Lawrence Berkeley Lab, California Univ., Berkeley (USA), 1980.
- [16] T. Hiraoka and H. Bichsel. Stopping powers and ranges for heavy ions. *Jpn. J. Med. Phys.*, 15:91, 1995.
- [17] ICRU Report 49. *Stopping powers and ranges for protons and alpha particles*. International Commission on Radiation Units and Measurements, Bethesda, Maryland, 1993.
- [18] Niels Bassler, Oliver Jäkel, Christian Skou Søndergaard, and Jørgen B. Petersen. Dose- and LET-painting with particle therapy. *Acta Oncol.*, 49:1170–1176, 2010.
- [19] H. Bethe. Zur Theorie des Durchgangs schneller Korpuskularstrahlen durch Materie. *Ann. Phys.*, 5:325, 1930.
- [20] H. Bethe. Bremsformel für Elektronen relativistischer Geschwindigkeit. *Z. Phys.*, 76:293, 1932.
- [21] N. Bohr. The penetration of atomic particles through matter. *Kgl. Danske Videnskab. Selskab Mat.-Fys. Medd.*, 18(8), 1948. This reference has long been difficult to obtain, but can now be downloaded from: http://www.sdu.dk/Bibliotek/E-hotel/MatFys.aspx?sc_lang=en.
- [22] U. Fano. Penetration of protons, alpha particles, and mesons. *Annu. Rev. Nucl. Sci.*, 13:1, 1963.
- [23] J. Lindhard and M. Scharff. Energy dissipation by ions in the keV region. *Phys. Rev.*, 124(1):128–130, 1961.
- [24] ICRU Report 37. *Stopping powers for electrons and positrons*. International Commission on Radiation Units and Measurements, Bethesda, Maryland, 1984.
- [25] Florian Sommerer, Katia Parodi, Alfredo Ferrari, Karin Poljanc, Wolfgang Enghardt, and Hannes Aiginger. Investigating the accuracy of the FLUKA code for transport of therapeutic ion beams in matter. *Phys. Med. Biol.*, 51:4385–4398, 2006.
- [26] W. H. Bragg and R. Keeman. On the alpha particles of radium and their loss of range in passing through various atoms and molecules. *Philos. Mag.*, 10:318–340, 1905.
- [27] Oksana Geithner. *Monte Carlo simulations for heavy ion dosimetry*. PhD thesis, University of Heidelberg, Germany, 2006.
- [28] Dževad Belkić. Review of theories on ionization in fast ion-atom collisions with prospects for applications to hadron therapy. *J. Math. Chem.*, 47:1366, 2010.
- [29] David C. Hansen, Armin Lühr, Nikolai Sobolevsky, and Niels Bassler. Benchmarking nuclear models in shield-hit. in preparation.
- [30] M. Krämer, O. Jäkel, T. Haberer, G. Kraft, D. Schardt, and U. Weber. Treatment planning for heavy-ion radiotherapy: physical beam model and dose optimization. *Phys. Med. Biol.*, 45:3299–3317, 2000.
- [31] M. Krämer and M. Scholz. Treatment planning for heavy-ion radiotherapy: calculation and optimization of biologically effective dose. *Phys. Med. Biol.*, 45:3319–3330, 2000.
- [32] Uli Weber and Gerhard Kraft. Design and construction of a ripple filter for a smoothed depth dose distribution in conformal particle therapy. *Phys. Med. Biol.*, 44:2765–2775, 1999.
- [33] Niels Bassler, Ioannis Kantemiris, Julia Engelke, Michael Holzscheiter, and Jørgen B. Petersen. Comparison of optimized single and multifield irradiation plans of antiproton, proton and carbon ion beams. *Radiother. Oncol.*, 95:87–93, 2010.
- [34] Helmut Paul and Andreas Schinner. Empirical stopping power tables for ions from ${}^3\text{Li}$ to ${}^{18}\text{Ar}$ and from 0.001 to 1000 MeV/nucleon in solids and gases. *At. Data Nucl. Data Tables*, 85:377, 2003. Available from <http://www-nds.iaea.or.at/stoppinggraphs/>.
- [35] M. J. Berger, J. S. Coursey, M. A. Zucker, and J. Chang. ESTAR, PSTAR, and ASTAR: Computer programs for calculating stopping-power and range tables for electrons, protons, and helium ions

- (version 1.2.3), 2005. [Online] Available: <http://physics.nist.gov/Star> [26 November 2018].
- [36] Jakob Toftegaard, Armin Lühr, and Niels Bassler. *libdedx*, 2010. [Online] Available: <http://sourceforge.net/projects/libdedx/> [26 November 2018].
- [37] Armin Lühr, Jakob Toftegaard, Ioannis Kantemiris, and Niels Bassler. Stopping power: the generic library libdedx and a study of clinically relevant stopping-power ratios for different ions. in preparation.
- [38] T. Elsässer, A. Gemmel, M. Scholz, D. Schardt, and M. Krämer. The relevance of very low energy ions for heavy-ion therapy. *Phys. Med. Biol.*, 54(7):N101, 2009.
- [39] F. Hubert, Rimbot R., and H. Gauvin. Semi-empirical formulae for heavy ion stopping powers in solids in the intermediate energy range. *Nucl. Instrum. Methods Phys. Res. B*, 36:357, 1989.
- [40] Jens Lindhard and Allan H. Sørensen. Relativistic theory of stopping for heavy ions. *Phys. Rev. A*, 53:2443, 1996.
- [41] David C. Hansen, Armin Lühr, Nikolai Sobolevsky, and Niels Bassler. SHIELD-HIT 10A, 2010. [Online] latest status: <http://aptg-trac.phys.au.dk/shieldhit> [26 November 2018].
- [42] Peter Sigmund, 2010. Private communication.
- [43] Harald Paganetti. Dose to water versus dose to medium in proton beam therapy. *Phys. Med. Biol.*, 54(14):4399, 2009.